Title: Bimodal crystallization rate curves of a molecular liquid with field-induced polymorphism

Author: Daniel M. Duarte, Ranko Richert, Karolina Adrjanowicz

Citation style: Duarte Daniel M., Richert Ranko, Adrjanowicz Karolina. (2021). Bimodal crystallization rate curves of a molecular liquid with field-induced polymorphism. „Journal of Molecular Liquids" (Vol. 342, 2021, art. no. 117419, s. 1-5), DOI:10.1016/j.molliq.2021.117419

Journal of Molecular Liquids 342 (2021) 117419

Contents lists available at ScienceDirect

Journal of Molecular Liquids

journal homepage: www.elsevier.com/locate/molliq

Bimodal crystallization rate curves of a molecular liquid with Field-Induced polymorphism

D.M. Duarte [a,b,*], R. Richert [c], K. Adrjanowicz [a,b,*]

[a] Institute of Physics, University of Silesia, 75 Pulku Piechoty 1, Chorzow 41-500, Poland
[b] Silesian Center for Education and Interdisciplinary Research (SMCEBI), 75 Pulku Piechoty 1, Chorzow 41-500, Poland
[c] School of Molecular Sciences, Arizona State University, Tempe, AZ 85287, USA

ARTICLE INFO

Article history:
Received 30 June 2021
Revised 26 August 2021
Accepted 27 August 2021
Available online 30 August 2021

ABSTRACT

In this study, we use dielectric spectroscopy to explore how frequency and amplitude of an applied strong electric field affect the overall crystallization kinetics over a range of temperatures, focusing on a molecular system with field-induced polymorphism: vinyl ethylene carbonate (VEC). The volume fraction of the field-induced polymorph can be controlled by the parameters of the high-electric field, i.e., frequency and amplitude. We find that the crystallization rate maximum of the field induced polymorph is located at lower temperatures relative to the that of the regular polymorph. The temperature of the highest crystallization rate for the regular polymorph was found to be unaffected by the electric field, but the overall rates increase with increasing field amplitude. The dimensionality of crystal growth is also analyzed via the Avrami parameter and is frequency invariant but affected by the field amplitude. Our results demonstrate that a detailed knowledge of the influence of high fields on crystallization facilitates control over the crystallization behavior and the final product outcome of molecular systems, providing new opportunities for material engineering and improving pharmaceuticals.

1. Introduction

If a liquid is supercooled to a sufficiently low temperature and rapidly enough, it can avoid crystallization and reach a glassy state. In this regime, the system is far from thermodynamic equilibrium and tends to rearrange itself in the well-defined array of atoms/-molecules of a crystal structure. A complete understanding of the crystallization process is a fundamental goal since the numerous properties of the final product depend on the degree of crystallinity, polymorphism, grain size, or crystal quality.[1–3]

Different factors can affect crystallization. An elementary guide to the crystal formation and description of its relation to the glassy state comes from the classical theories of nucleation and growth. [4,5] In a classical view, the crystallization process involves forming an embryonic nucleus and its subsequent growth. The rates of nucleation, $J(T)$, and crystal growth, $u(T)$, are subject to distinct temperature profiles, but each process typically reaches its maximum at some temperature between glass transition at T_g and the melting point at T_m. The temperature of the highest crystal growth rate (u) is usually above that of the nucleation rate (J). The temperature zone in which $u(T)$ and $J(T)$ curves overlap considerably leads to ideal conditions for fast crystallization, especially on cooling the melt.[6,7]

Several experimental, as well as theoretical studies, have revealed that sufficiently high electric fields affect crystallization. [5,8–17] However, predicting how the electric field will affect the crystallization is not fully established. In a classical view, the electric field affects both nucleation (J) and crystal growth (u):[18,19]

$$J \propto D \exp\left(-\Delta G_c(E)/k_B T\right) \tag{1}$$

$$u \propto D[1 - \exp\left(-\Delta\mu(E)/k_B T\right)] \tag{2}$$

where D is a diffusion constant, ΔG_C is the Gibbs free energy, and $\Delta\mu$ is the difference in chemical potentials between melt and crystal phase. Both ΔG_C and $\Delta\mu$ will be affected by the electric field, also making J and u dependent on the electric field. Still, the information needed to predict the magnitude of the field on the crystallization is generally not available. In the case of polar liquids, the modifications of thermodynamic potentials[20–22], free energy and entropy, and the field-induced orientation[23,24] induced by high electric fields can have an enormous impact due to the possibility of leading the final product into a different polymorph.[17,18]

A single component glass-forming liquid with a relatively large value of the permanent dipole moment[25], vinyl ethylene carbonate (VEC), a vinyl derivative of propylene carbonate (PC), has been studied recently under high electric fields. [9,17,18,26] It was

* Corresponding authors.
E-mail addresses: daniel.duarte@smcebi.edu.pl, dduarte@us.edu.pl (D.M. Duarte).

https://doi.org/10.1016/j.molliq.2021.117419
0167-7322/

shown that the crystallization time is shortened and/or a completely new polymorphic form can be obtained when a high electric field is applied. Additionally, it was found that these electric field effects are influenced by the frequency and magnitude of the applied electric field.

Despite the research previously done, there is no predictive theory or experimental evidence that addressed how the high-electric field influences the crystallization rate curves. This work steps forward on resolving this question by exploring how the electric field affects the crystallization behavior of VEC for different temperatures and for different volume fractions of the field-induced polymorph after crystallization has been completed. For a wide range of crystallization temperatures, T_c, VEC is subjected to different magnitudes and frequencies of alternating (AC) or static (DC) high fields. We analyze the Avrami parameters (rate k, exponent n) of the crystallization kinetics and subsequently record the melting profiles of the final crystallized product. This facilitates disentangling the crystallization curves $k(T_c)$ for the two polymorphs, the regular and the field-induced ones, in a more wide temperature range. The results presented in this work yield valuable information about the effects of the electric field on the crystallization rate curve, completing a study on the influence of the electric field on the crystallization of the VEC.

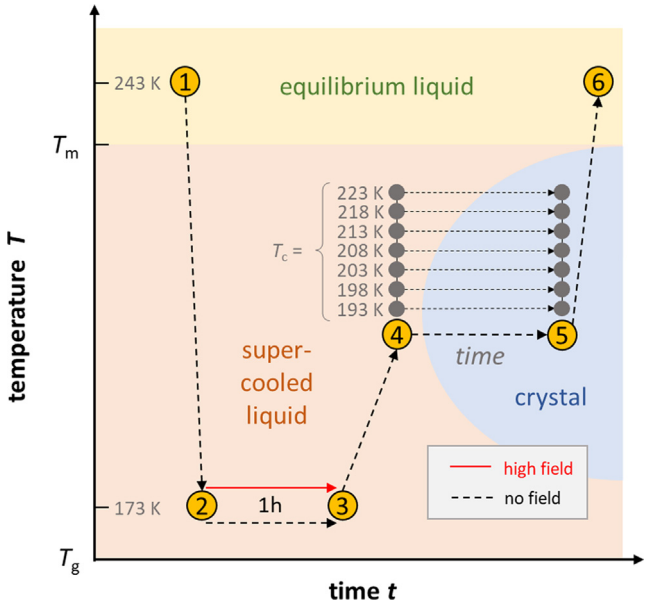

Fig. 1. Overview of the experimental protocol used to study the effect of the magnitude and frequency of the field on the crystallization of VEC at different crystallization temperatures, T_c.

2. Experimental

The compound 4-vinyl-1,3-dioxolan-2-one or vinyl ethylene carbonate (VEC, purity 99%) was obtained from Sigma-Aldrich and used as received. The liquid was loaded into two parallel polished stainless-steel electrodes separated by a Teflon ring of d = 25 μm nominal thickness, leaving an active inner electrode surface area of r = 7 mm radius. The resulting geometric capacitance is $C_{geo} = \varepsilon_0 \pi r^2/d = 54.5$pF. By comparing the observed permittivity with reference data, the actual electrode separation was determined to be closer to 20 μm. A Novocontrol Quatro temperature control system was responsible for regulating the temperature of the sample cell with stability better than 0.1 K.

The dielectric measurements were carried out in the frequency range from 10^{-1} to 10^4 Hz using a Novocontrol Alpha Analyzer. The high voltage unit HVB1000 from Novocontrol was used to achieve the high electric fields. This extension test interface boosts the voltages of the Alpha Analyzer from 40 V_{peak} to 500 V_{peak}. All voltage and field amplitudes are reported as root-mean-square (RMS) values. All fields intended to affect crystallization were around $E \approx 80$ kV cm^{-1}, while amplitudes of the alternating fields used to measure dielectric permittivity, ε, in the linear regime were kept below 16 kV cm^{-1}, which is a factor of ≈ 25 lower in terms of nonlinear ($\sim E^2$) effects.

3. Results and discussion

To identify the influence of the magnitude and frequency of the electric field on the crystallization of VEC at different temperatures, we have followed the thermal protocol shown in Fig. 1. This experiment starts at the temperature T = 243 K, which is 15 K above the melting temperature of the low-field polymorph and thus ensures an equilibrated state. In the next step, the sample is cooled down to T = 173 K (=T_g + 2 K) with a rate of approximately 10 K min^{-1}. The sample is exposed to the desired high field, DC or AC, for 1 h at this temperature. For reference, experiments at zero field were also performed. Thereupon, the temperature of the sample is increased to the crystallization temperature, located between 193 K and 223 K, at a rate of approximately 5 K min^{-1}. The progress of the crystallization is followed using dielectric spectroscopy, that is, by analyzing the drop of the dielectric permittivity at 10 kHz with time. After crystallization, the sample was heated at a constant rate of 1 K min^{-1} to T = 245 K, and the melting behavior is followed by measuring the dielectric permittivity at 10 kHz during this heating ramp. Due to the high conductivity of the sample at elevated temperatures and the resulting risk of sample failure, it is not possible to follow a different experimental procedure where high fields are applied during crystallization.

After increasing the temperature from T = 173 K to the desired crystallization temperature in the absence of a field, the crystallization progress can be monitored by analyzing the changes in the real part of dielectric permittivity using dielectric spectroscopy. In polar liquids, the dielectric constant is dominated by polarization due to rotational motion of permanent dipoles. However, these motions are suppressed when the sample is crystallized, making it possible to follow the crystallization process using dielectric techniques. Therefore, as a good approximation, ε' measures the fraction of crystal (V_{cry}/V_{total}) through[18,27,28]

$$V_{cry}/V_{total} = (\varepsilon_s - \varepsilon')/(\varepsilon_s - \varepsilon_\infty) \quad (3)$$

where ε_s is the dielectric constant of the liquid and ε_∞ is considered the permittivity of the crystalline state and of the liquid in the high frequency limit, in which orientational contributions from permanent dipoles are absent. The volume fraction can be related to the rate of crystallization, k, and the Avrami parameter, n, which represents the dimensionality and geometry of the crystal growth through the Avrami relation [29,30]

where t is the time after the onset of crystallization, i.e., excluding the incubation time of the process. In cases where both crystal types are formed, the superposition of two Avrami curves may be expected to be required to fit the crystallization behavior. Instead, we observe, as previously, [9,17,18,26] that a single Avrami fit provides a good representation of the data. If the two crystal types lead to distinct Avrami curves, their difference cannot be resolved on the basis of the present data.

3.1. Crystallization rates

In Fig. 2a, we present the temperature dependence of k as measured between T_c = 193 K and 223 K using an AC field

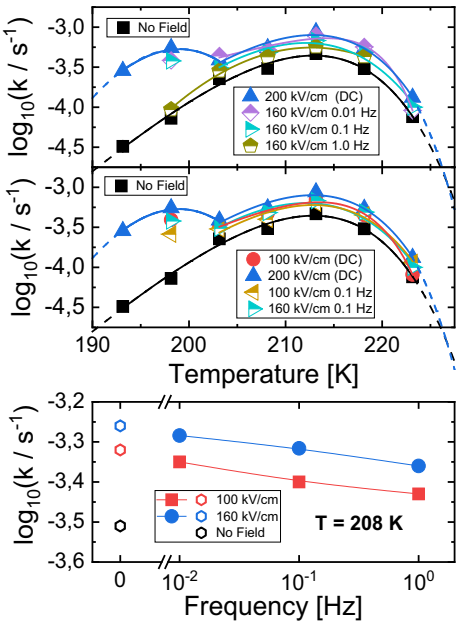

Fig. 2. The characteristic time of crystallization for VEC plotted as a function of crystallization temperature using different field magnitudes (a) $E = 200$ kV cm^{-1} for a DC field and $E = 160$ kV cm^{-1} for an AC field with different frequencies; (b) $E = 200$ and 100 kV cm^{-1} for a DC field and $E = 160$ and 100 kV cm^{-1} for an AC field at fixed frequency, $f = 10^{-1}$ Hz. Solid lines are fits to the experimental data with the use of an exponential function plus a linear term. Panel (c) shows the frequency dependence of the crystallization rate when using AC fields. The values obtained in the absence of high-field and for DC case were added as a reference.

($E = 160$ kV cm^{-1}) of different frequencies. For the crystallization experiments where no field was applied, the logarithmic crystallization rate increases from − 4.49 at 193 K to − 3.33 at 213 K and then decreases again at higher temperatures. In this way, the most favorable temperature region for crystallization is within the 210–220 K range, as indicated by the maximum of the crystallization rate curve. For the highest field frequency that we use, i.e., 1 Hz, we do not observe any changes in the overall crystallization rate curve position, but a uniform increment in the crystallization rate can be observed if compared to the zero field case.

The crystallization rate behavior, $k(T_c)$, for the case where we use the same field amplitude, 160 kV cm^{-1}, but at a lower frequency, $f = 0.1$ Hz, shows a qualitative difference compared with the $f = 1$ Hz situation. At $T_c = 198$ K and below, instead of the value of k further decreasing, the rate increases and gives rise to another crystallization maximum located at lower temperatures. This new maximum is due to the field-induced polymorph generated for frequencies below a specific threshold and with sufficient magnitude of the field.[9,26] For higher temperatures, $T_c \geq 203$ K, the same field parameters result only in an increase of the magnitude of the crystallization rate. For an even lower frequency, $f = 10^{-2}$ Hz, we also observe two crystallization rate maxima, see Fig. 2a, but with a somewhat higher rate k at low temperatures relative to the $f = 0.1$ Hz cases. Likewise, for the crystallization curve associated with higher temperatures, the rates also increase with lowering the frequency, while its maximum position is largely maintained. The DC- field, $f = 0$, promotes the optimal formation rate of the new polymorph, consistent with the frequency dependence discussed above.

The dependence of k with the magnitude of the electric field is presented in Fig. 2b. For the case of the AC field, the chosen fixed frequency was $f = 0.1$ Hz. At this frequency, it is possible to generate the field-induced polymorph. For both field magnitudes, 100 and 160 kV cm^{-1}, it is possible to observe two crystallization rate maxima, associated with the field-induced and ordinary polymorphs, at low and higher temperatures, respectively. The magnitude of the crystallization rate increases with higher field amplitudes; however, the temperature position of the maximum remains unchanged. Likewise, for DC values, with field magnitudes of 100 and 200 kV cm^{-1}, it is possible to observe the crystallization maxima associated with both polymorphs. Comparing both curves, we observe that the maximum of the crystallization curve remains unchanged; however, the rates increase with increasing the field magnitude. A closer look at the influence of the magnitude and frequency of the high electric field on crystallization rate k is presented in Fig. 2c. At the selected temperature, $T_c = 208$ K, we can observe that with increasing the field magnitude the crystallization rate for both AC and DC fields increases. Moreover, in the AC case, the frequency also has an essential role in controlling the crystallization rate. For lower frequencies, the values of k are higher and approach the levels observed with DC fields.

Overall, the position of the crystallization rate maximum is independent of the magnitude and frequency of the applied field. However, these factors can promote crystallization progress. For example, increasing the amplitude of the applied field, or in AC case, decreasing the frequency of the applied field can increase the crystallization rate. Moreover, at lower temperatures (i.e., closer to the glass transition), it is possible to generate a new polymorph when using sufficiently low frequencies or higher field amplitudes. The crystallization rate, also in this case, will depend on the amplitude and frequency of the applied field. As for the separation of these crystallization curves associated with the two polymorphs, the contribution of the ordinary polymorph with a higher maximum position is expected to reflect $u(T)$, as previous studies have shown the absence of nucleation for $T \geq 198$ K.[26] The lower temperature contribution associated with the field-induced polymorph will reflect a mix of $J(T)$ and $u(T)$, since that polymorph can be nucleated at high fields around $T = 198$ K.

3.2. Avrami analysis

Applying a high-electric field not only affects the crystallization time but also influences the dimensionality of growing crystals. These changes can be tracked using the Avrami parameter, n, see Eq. (4). The evolution of n as a function of temperature is plotted in Fig. 3a and 3b for different field frequencies and amplitudes, respectively. As can be seen, the Avrami parameter increases with increasing the temperature, changing from $n \approx 2$ at lower temperatures to $n \approx 3.5$ at higher temperatures in the case of zero field. When using 200 kV cm^{-1} (DC), the n value at $T_c = 193$ K is similar to the zero field case, while with increasing the temperature it increases to $n \approx 4$. This suggests that the crystallites adopt a rod-like morphology and grow from instantaneously formed nuclei at lower temperatures, while at higher temperatures, its growth progresses in a spherical way with a sporadic nucleation event. It is observed that increasing the field magnitude will affect the Avrami parameter. The n values are higher when increasing the magnitude of the electric field, both AC and DC. Interestingly, as we observe in Fig. 3b, the frequency of the AC field does not influence the dimensionality of growing crystals in the present temperature range.

In Fig. 3c, we can observe in more detail, for a selected temperature, $T_c = 213$ K, that the Avrami parameter depends on the magnitude of the applied electric field. Specifically, it increases as the amplitude of the field increases, whereas it does not change significantly when the field frequency is changed. The field frequency should affect more the crystallization rate, as observed in a previous paper.[26] However, in the present experimental protocol, the field is applied at a low temperature, $T = 173$ K, and the crystallization progresses in the absence of a strong field. Herewith, the particles are not forced to be oriented due to the presence of the field,

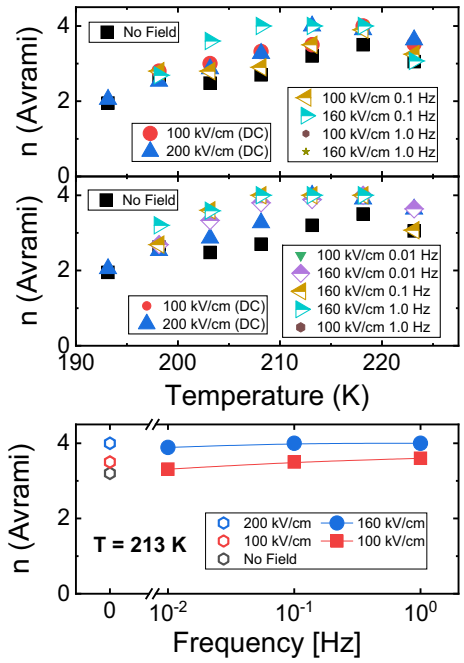

Fig. 3. The Avrami parameter for VEC plotted as a function of crystallization temperature at (a) $E = 200$ kV cm^{-1} for DC field and $E = 160$ kV cm^{-1} for AC field with different frequencies; (b) $E = 200$ kV cm^{-1} and 100 kV cm^{-1} for DC field and $E = 160$ and 100 kV cm^{-1} for AC field at 10^{-1} Hz; Panel (c) shows the evolution of crystallization rate as a function of the frequency of the used AC field. The values obtained in the absence of high-field and for DC case were added for reference. Error bars for n are no included, as they do not exceed the symbol size in this graph.

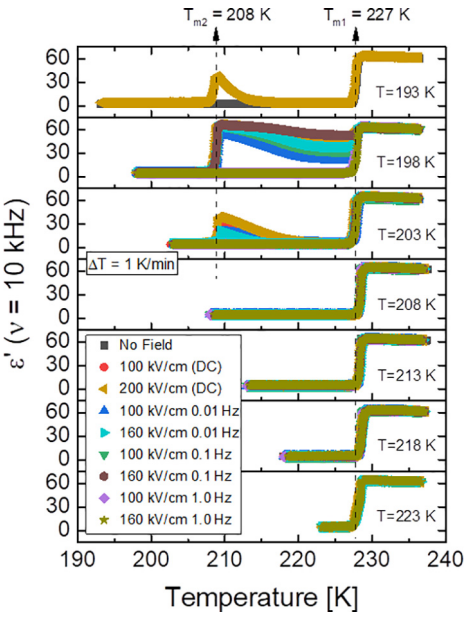

Fig. 4. Melting curves of previously crystallized VEC analyzed in terms of the permittivity ε' measured at a frequency $\nu = 10$ kHz upon scanning temperature from the crystallization temperature to 245 K at a rate of 1 K min^{-1}. Crystallization has been field-induced using different magnitudes and frequencies of the field, as indicated in the legends. The zero field crystallization counterpart is added for reference.

contrary to what happens when there is a high field applied with the crystallization ongoing.

It is highly desirable to come to a more molecular understanding of the interplay between the effect of the external field and crystallization temperature. The frequency dependence pointed toward the field-induces crystal nuclei being macroscopically polarized but a crystal structure analysis in needed in order to gain a better understanding, which is not available because ex-situ studies are not easily possible with sub-ambient melting temperatures.

3.3. Melting behavior

After the crystallization is completed, the melting process was followed in the absence of a high electric field to verify the final product. The melting curves measured at $f = 10$ kHz, at a rate of $\Delta T = 1$ K min^{-1}, are shown in Fig. 4, for all crystallization temperatures of this study. In the case when no high electric field was applied, we can observe only the formation of one polymorph with melting temperature $T_{m1} \approx 227$ K. Similar to the non-field case, when the AC field is applied with $f = 1$ Hz and magnitude of 100 or 160 kV cm^{-1}, only one melting event is detected, associated with the regular polymorph. However, for a crystallization temperature of $T_c = 198$ K, with the frequency of the AC field decreased to $f = 10^{-1}$ or 10^{-2} Hz, we observe an additional melting event at $T_{m2} \approx 208$ K, associated with the field-induced polymorph. Intuitively, melting at T_{m2} is associated with the crystallization event taking place at lower temperatures, as observed in Fig. 2a and 2b. The transition at 208 K is identified as melting of the high-field crystal, as the process recovers the orientational degrees of freedom characteristic of the liquid state. The process is thus incompatible with a solid–solid transition, which would not be associated with recovering the static dielectric constant of the pure liquid state. The subsequent crystallization above 208 K is the result of residual nuclei of the stable type I crystals, and the melting event at 208 K also occurs in the absence of recrystallization (see for more details [17]). The intensity of the ε' peak near T_{m2}, which can be associated with the volume fraction of the metastable polymorph, increases when using the AC field frequency of $f = 10^{-2}$ Hz compared with $f = 10^{-1}$ Hz. At $T_c = 203$ K, only the frequency $f = 10^{-2}$ Hz can produce the field-induced polymorph, while in the case of $f = 10^{-1}$ Hz, there are no traces associated with the high-field polymorph melting recorded in the dielectric temperature scans. All other melting curves associated with crystallization temperatures between 208 K and 223 K follow the same behavior as the no-field case, showing only the ordinary polymorph which melts at T_{m1}.

The influence of the magnitude of the high electric field on the final product composition can be observed in the melting events. For example, in Fig. 4, at $T_c = 198$ K, for frequencies $f = 10^{-1}$ Hz and $f = 10^{-2}$ Hz, we observe that the intensity of dielectric permittivity is higher when using 160 kV cm^{-1} in comparison with 100 kV cm^{-1}. The same can be observed at $T_c = 203$ K, for $f = 10^{-2}$ Hz, the melting event is more intense when the field magnitude increases. A higher value of the dielectric permittivity at T_{m2} indicates that the fraction of the high-field polymorph obtained in the crystallized material was greater in such cases. Likewise, when the DC field is used, we observe two melting events for crystallization temperatures between $T_c = 193$ K and $T_c = 203$ K, while for the remaining temperatures, only one melting event at T_{m1} is observed. Similar to the AC field, the magnitude of the DC high-field affects the quantity of formed polymorph. At $T_c = 198$ K and $T_c = 203$ K, when the magnitude of the field was 200 kV cm^{-1} shows a higher intensity of the ε' in comparison to when the field magnitude used was 100 kV cm^{-1}. All the remaining temperatures, between $T_c = 208$ K to $T_c = 223$ K, show the same behavior as the zero field case.

4. Conclusions

In this work, the effect of the high-electric field on the crystallization of polar molecular liquid was explored, with focus on the crystallization rate in a wide temperature range. First, the electric field was only applied close to T_g, and then the sample was heated up to the desired crystallization temperature, T_c. We have shown that the frequency and amplitude of the applied AC high-field allow forming at lower temperatures one additional crystallization curve maximum, related to the formation of the field-induced polymorph with distinct melting temperature. Moreover, increasing the magnitude or decreasing the frequency of the applied field will increase the crystallization rate of this polymorph. Likewise, a high DC field influences the crystallization in the same manner as an AC field of very low frequency. However, these factors do not affect the position of the crystallization rate maxima. Additionally, the melting curves show that the quantity of the field-induced polymorph in the final crystalline material can be controlled by changing the magnitude or frequency of the field. Finally, the Avrami parameter n was found to be affected by the magnitude of both DC and AC electric fields or by the temperature at which crystallization occurs, while it seems to be independent of the frequency of the applied AC field.

This work sums up the study of how AC and DC fields can influence the crystallization behavior of VEC using dielectric spectroscopy. Together with previous reports,[9,17,18,26] it provides a complete picture of how to control or suppress specific polymorphs by using the frequency or amplitude of the applied field, potentially useful in materials engineering or the pharmaceutical industry. Unfortunately, it is not possible to study the final crystallization product of VEC in more detail due to its low melting point, which limits the options of in-situ studies of the structure. The sub-ambient melting point (-35 °C) of the crystals prevent a direct characterization of their crystal structure and molecular properties. This is especially true for the field-induced polymorph. We aim to conduct such studies for a field induced polymorph for which the melting point is above room temperature. However, our results collected for VEC still provide an essential experimental guide that can be used for more advanced future studies, aimed at applying a high electric field to control the crystallization behavior of molecular materials.

Declaration of Competing Interest

The authors declare that they have no known competing financial interests or personal relationships that could have appeared to influence the work reported in this paper.

Acknowledgment

Part of this work was supported by the National Science Foundation under grant no. DMR-1904601. Financial support from the National Science Centre within the framework of the SONATA BIS project (Grant No. 2017/26/E/ST3/00077) is greatly acknowledged.

References

[1] J. Haleblian, W. McCrone, Pharmaceutical Applications of Polymorphism, J. Pharm. Sci. 58 (8) (1969) 911–929, https://doi.org/10.1002/jps.2600580802.
[2] N. Rodríguez-hornedo, D. Murphy, Significance of Controlling Crystallization Mechanisms and Kinetics in Pharmaceutical Systems, *J Pharmaceutical Sci*. Am Chem Soc July 1 88 (7) (1999) 651–660, https://doi.org/10.1021/js980490h.
[3] A. Lendlein, S. Kelch, Shape-Memory Polymers. *Angew. Chemie Int. Ed.* 41 (12) (2002) 2034, https://doi.org/10.1002/1521-3773(20020617)41:12<2034::AID-ANIE2034>3.0.CO;2-M.
[4] R. Becker, W. Döring, Kinetische Behandlung Der Keimbildung in Übersättigten Dämpfen, Ann. Phys. 416 (8) (1935) 719–752, https://doi.org/10.1002/(ISSN)1521-388910.1002/andp.v416:810.1002/andp.19354160806.
[5] I.S. Gutzow, J.W.P. Schmelzer (Eds.), The Vitreous State, Springer Berlin Heidelberg, Berlin, Heidelberg, 2013.
[6] J.A. Baird, B. Van Eerdenbrugh, L.S. Taylor, A Classification System to Assess the Crystallization Tendency of Organic Molecules from Undercooled Melts, J. Pharm. Sci. 99 (9) (2010) 3787–3806, https://doi.org/10.1002/jps.22197.
[7] N.S. Trasi, L.S. Taylor, Effect of Polymers on Nucleation and Crystal Growth of Amorphous Acetaminophen, CrystEngComm 14 (16) (2012) 5188, https://doi.org/10.1039/c2ce25374g.
[8] G.J. Evans, Crystal Growth in Electric Fields, Mater. Lett. 2 (5) (1984) 420–423, https://doi.org/10.1016/0167-577X(84)90153-8.
[9] D.M. Duarte, R. Richert, K. Adrjanowicz, Frequency of the AC Electric Field Determines How a Molecular Liquid Crystallizes, J. Phys. Chem. Lett. 11 (10) (2020) 3975–3979, https://doi.org/10.1021/acs.jpclett.0c01002.
[10] K. Kotsuki, S. Obata, K. Saiki, Electric-Field-Assisted Position and Orientation Control of Organic Single Crystals, Langmuir 30 (47) (2014) 14286–14291, https://doi.org/10.1021/la503286y.
[11] C. Parks, A. Koswara, H.-H. Tung, N. Nere, S. Bordawekar, Z.K. Nagy, D. Ramkrishna, Molecular Dynamics Electric Field Crystallization Simulations of Paracetamol Produce a New Polymorph, Cryst. Growth Des. 17 (7) (2017) 3751–3765, https://doi.org/10.1021/acs.cgd.7b0035610.1021/acs.cgd.7b00356.s001.
[12] M. Taleb, C. Didierjean, C. Jelsch, J. Mangeot, B. Capelle, A. Aubry, Crystallization of Proteins under an External Electric Field, J. Cryst. Growth 200 (3–4) (1999) 575–582, https://doi.org/10.1016/S0022-0248(98)01409-2.
[13] Z. Hammadi, S. Veesler, New Approaches on Crystallization under Electric Fields, Prog. Biophys. Mol. Biol. 101 (1–3) (2009) 38–44, https://doi.org/10.1016/j.pbiomolbio.2009.12.005.
[14] C.N. Nanev, A. Penkova, Nucleation of Lysozyme Crystals under External Electric and Ultrasonic Fields, J. Cryst. Growth 232 (1–4) (2001) 285–293, https://doi.org/10.1016/S0022-0248(01)01169-1.
[15] J.E. Aber, S. Arnold, B.A. Garetz, A.S. Myerson, Strong Dc Electric Field Applied to Supersaturated Aqueous Glycine Solution Induces Nucleation of the γ Polymorph, Phys. Rev. Lett. 94 (14) (2005), https://doi.org/10.1103/PhysRevLett.94.145503 145503.
[16] G. Di Profio, M.T. Reijonen, R. Caliandro, A. Guagliardi, E. Curcio, E. Drioli, Insights into the Polymorphism of Glycine: Membrane Crystallization in an Electric Field, Phys. Chem. Chem. Phys. 15 (23) (2013) 9271, https://doi.org/10.1039/c3cp50664a.
[17] K. Adrjanowicz, M. Paluch, R. Richert, Formation of New Polymorphs and Control of Crystallization in Molecular Glass-Formers by Electric Field, Phys. Chem. Chem. Phys. 20 (2) (2018) 925–931, https://doi.org/10.1039/C7CP07352F.
[18] K. Adrjanowicz, R. Richert, Control of Crystallization Pathways by Electric Fields. In *Dielectrics and crystallization*, Springer (2020) 149–167, https://doi.org/10.1007/978-3-030-56186-4_6.
[19] J.W.P. Schmelzer, Crystal Nucleation and Growth in Glass-Forming Melts: Experiment and Theory, J. Non. Cryst. Solids 354 (2–9) (2008) 269–278, https://doi.org/10.1016/j.jnoncrysol.2007.06.103.
[20] D. Kashchiev, Nucleation in External Electric Field, J. Cryst. Growth 13–14 (C) (1972) 128–130, https://doi.org/10.1016/0022-0248(72)90074-7.
[21] D. Kashchiev, On the Influence of the Electric Field on Nucleation Kinetics, Philos. Mag. 25 (2) (1972) 459–470, https://doi.org/10.1080/14786437208226816.
[22] J.O. Isard, Calculation of the Influence of an Electric Field on the Free Energy of Formation of a Nucleus, Philos. Mag. 35 (3) (1977) 817–819, https://doi.org/10.1080/14786437708236010.
[23] E. Gattef, Y. Dimitriev, Reversible Monopolar Switching in Vanadium-Tellurite Glass Threshold Devices, Philos. Mag. B 40 (3) (1979) 233–242, https://doi.org/10.1080/13642817908246373.
[24] E. Gattef, Y. Dimitriev, Nucleation Theory of Threshold Switching in Vanadate-Glass Devices, Philos. Mag. B 43 (2) (1981) 333–343, https://doi.org/10.1080/13642818108221903.
[25] A. Jedrzejowska, Z. Wojnarowska, K. Adrjanowicz, K.L. Ngai, M. Paluch, Toward a Better Understanding of Dielectric Responses of van Der Waals Liquids: The Role of Chemical Structures, J. Chem. Phys. 146 (9) (2017) 094512, https://doi.org/10.1063/1.4977736.
[26] D.M. Duarte, R. Richert, K. Adrjanowicz, AC versus DC Field Effects on the Crystallization Behavior of a Molecular Liquid, Vinyl Ethylene Carbonate (VEC), Phys. Chem. Chem. Phys. 23 (1) (2021) 498–505, https://doi.org/10.1039/D0CP05290F.
[27] J. Mijovic, J.-W. Sy, T.K. Kwei, Reorientational Dynamics of Dipoles in Poly (Vinylidene Fluoride)/Poly(Methyl Methacrylate) (PVDF/PMMA) Blends by Dielectric Spectroscopy, Macromolecules 30 (10) (1997) 3042–3050, https://doi.org/10.1021/ma961774w.
[28] M.H. Jensen, C. Alba-Simionesco, K. Niss, T. Hecksher, A Systematic Study of the Isothermal Crystallization of the Mono-Alcohol n-Butanol Monitored by Dielectric Spectroscopy, J. Chem. Phys. 143 (13) (2015) 134501, https://doi.org/10.1063/1.4931807.
[29] M. Avrami, Kinetics of Phase Change, I General Theory. *J. Chem. Phys.* 7 (12) (1939) 1103–1112, https://doi.org/10.1063/1.1750380.
[30] M. Avrami, Kinetics of Phase Change. II Transformation-Time Relations for Random Distribution of Nuclei, J. Chem. Phys. 8 (2) (1940) 212–224, https://doi.org/10.1063/1.1750631.